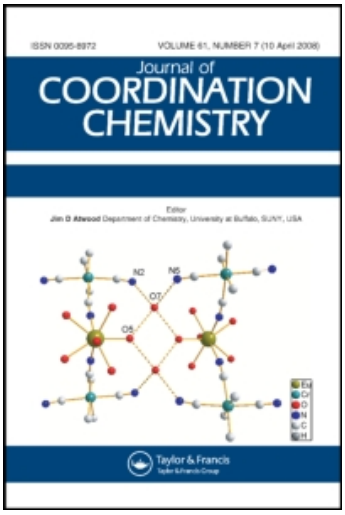

Journal of Coordination Chemistry
Publication details, including instructions for authors and subscription information:
http://www.informaworld.com/smpp/title~content=t713455674

Four 1,3-bis(1,2,4-triazol-1-yl)propane-based metal complexes tuned by competitive coordination of mixed ligands: synthesis, solid structure, and fluorescence

Wen Feng[a]; Ruo-Nan Chang[a]; Jing-Yi Wang[a]; En-Cui Yang[a]; Xiao-Jun Zhao[a]
[a] Tianjin Key Laboratory of Structure and Performance for Functional Molecule, College of Chemistry and Life Science, Tianjin Normal University, Tianjin 300387, P.R. China

First published on: 20 October 2009

To cite this Article Feng, Wen , Chang, Ruo-Nan , Wang, Jing-Yi , Yang, En-Cui and Zhao, Xiao-Jun(2010) 'Four 1,3-bis(1,2,4-triazol-1-yl)propane-based metal complexes tuned by competitive coordination of mixed ligands: synthesis, solid structure, and fluorescence', Journal of Coordination Chemistry, 63: 2, 250 — 262, First published on: 20 October 2009 (iFirst)
To link to this Article: DOI: 10.1080/00958970903348437
URL: http://dx.doi.org/10.1080/00958970903348437

Journal of Coordination Chemistry
Vol. 63, No. 2, 20 January 2010, 250–262

Taylor & Francis
Taylor & Francis Group

Four 1,3-bis(1,2,4-triazol-1-yl)propane-based metal complexes tuned by competitive coordination of mixed ligands: synthesis, solid structure, and fluorescence

WEN FENG, RUO-NAN CHANG, JING-YI WANG, EN-CUI YANG and XIAO-JUN ZHAO*

Tianjin Key Laboratory of Structure and Performance for Functional Molecule, College of Chemistry and Life Science, Tianjin Normal University, Tianjin 300387, P.R. China

(*Received 9 June 2009; in final form 27 July 2009*)

Four 1,3-bis(1,2,4-triazol-1-yl)propane (btp)-based transition metal complexes, $\{[Zn(btp)_3]\cdot(ClO_4)_2\}_n$ (**1**), $[Zn(btp)_2(dca)_2]_n$ (**2**), $[Zn(btp)(NCS)_2]$ (**3**), and $[Mn(btp)_2(NCS)_2]_n$ (**4**), have been obtained by introducing small anionic coligands and structurally characterized by single crystal X-ray diffraction, elemental analysis, IR spectra, thermogravimetric curves, and solid luminescence spectra. Structural determinations reveal that the polymeric triple-stranded chain for **1** without coligand is changed into 1-D double-stranded chains for **2** and **4**, and discrete binuclear structure for **3**. Compared with **1**, the mixed-ligand complexes are moderately destabilized for **2** and **4**, and slightly enhanced for **3**. Additionally, the four solid complexes exhibit strong emissions, suggesting their potential applications as luminescent materials.

Keywords: 1,3-Bis(1,2,4-triazol-1-yl)propane; Mixed-ligand; Crystal structure; Fluorescent property

1. Introduction

Design and construction of bistriazole-based complexes are of considerable interest due to their intriguing architectures [1–5] and a large number of coordination polymers with bis(1,2,4-triazol-1-yl)alkanes ($n = 1, 2, 3, 4, 6$) has been reported [1–12]. The bis(1,2,4-triazol-1-yl)alkane has displayed two significant features, each ligand can act as an organic linker to aggregate different metal ions by bidentate bridging with size of the metallomacrocycle formed by metal ion and bridging bistriazole significantly increased with increment of the aliphatic chain. On the other hand, the functional linkers with variable length exhibit various conformations due to free rotation of the C–C single bond in the aliphatic chain, inducing diverse structures ranging from discrete binuclear structures to high-dimensional inter-penetrating metal organic frameworks [9b]. Obviously, the longer the aliphatic chain, the easier is the conformational transformation. Several different conformations (*trans–trans*, *trans–gauche*, *gauche–gauche*) can be observed even for a ligand with fixed-length aliphatic chain. Thus, the length of the

*Corresponding author. Email: xiaojun_zhao15@yahoo.com.cn

Journal of Coordination Chemistry
ISSN 0095-8972 print/ISSN 1029-0389 online © 2010 Taylor & Francis
DOI: 10.1080/00958970903348437

aliphatic chain plays an essential role for the structural motif of the complexes. Additionally, anions with controllable size and shape have been widely utilized as building blocks to tune the structural diversity of the flexible ligand-based coordination complexes. As a result, they can behave either as a guest species to fill in the cavities or as a hydrogen-bonding acceptor/donor to extend the higher dimensional structure, in addition to charge compensation. Some anions can act as coligands selectively coordinating mono-, bi-, or tridentate, forming mixed-ligand metal complexes [9, 10]. Recently, various 1,3-bis(1,2,4-triazol-1-yl)propane (btp)-based Cu^{II}, Fe^{II}, and Co^{II} complexes with different anions (ClO_4^-, $CF_3SO_3^-$, BF_4^-, NCS^-, $NCSe^-$) have been studied [1, 2, 6, 9]. Herein, to continue to investigate competitive binding of mixed anions on the architecture of coordination complexes, self-assembly of the flexible btp and Zn^{II}/Mn^{II} salts with different anions ClO_4^-, NCS^-, and dca^-, were carried out. Four complexes, $\{[Zn(btp)_3]\cdot(ClO_4)_2\}_n$ (**1**), $[Zn(btp)_2(dca)_2]_n$ (**2**), $[Zn(btp)(NCS)_2]$ (**3**), and $[Mn(btp)_2(NCS)_2]_n$ (**4**), were isolated and characterized by X-ray crystallography, elemental analysis, IR spectroscopy, thermogravimetric analysis, and fluorescent properties. Structural determinations reveal that the polymeric triple-stranded chain for **1** without coligand is changed into 1-D double-stranded chains for **2** and **4**, and discrete binuclear structure for **3**. Such structural transformation results from different coordination geometry of Zn^{II} and competitive binding between btp and auxiliary ligand. Luminescence and thermal stability of the resulting complexes are discussed.

2. Experimental

2.1. *Reagents and instruments*

The btp ligand was synthesized according to the literature [1] and all other starting materials were of reagent grade obtained from commercial sources and used as received. Fourier transform IR spectra (KBr pellets) were taken on an Avatar-370 (Nicolet, USA) spectrometer. Elemental analyses for C, H, and N were performed on a CE-440 (Leemanlabs, USA) analyzer. Thermogravimetric-differential thermogravimetric analysis experiments were carried out on a Shimadzu (Japan) simultaneous DTG-60A thermal analysis instrument with a heating rate of $8^\circ C\,min^{-1}$ from room temperature to 800°C under nitrogen (flow rate $10\,mL\,min^{-1}$). Fluorescence spectra of the polycrystalline samples were performed on a Cary Eclipse fluorescence spectrophotometer (Varian, USA) equipped with a xenon lamp and quartz carrier at room temperature.

2.2. *Synthesis of $\{[Zn(btp)_3](ClO_4)_2\}_n$ (1)*

To an aqueous solution (10 mL) of $Zn(ClO_4)_2\cdot 6H_2O$ (37.3 mg, 0.1 mmol) was slowly added a methanol solution (10 mL) containing btp (17.8 mg, 0.1 mmol) with constant stirring. After further stirring for 1 h, the mixture was filtered. Upon slow evaporation of the filtrate at room temperature, colorless block-shaped crystals suitable for X-ray diffraction were collected within 4 days (yield: 48% based on Zn^{II}). Anal. Calcd for $C_{3.50}H_5Cl_{0.33}N_3O_{1.33}Zn_{0.17}$: C, 31.56%; H, 3.78%; N, 31.55%. Found: C, 31.46%;

H, 3.82%; N, 31.50%. IR (KBr, cm^{-1}): 3131s, 1524vs, 1436m, 1378w, 1289s, 1213m, 1095br, 1003m, 880m, 676m, 620m, 482w.

2.3. *Synthesis of [Zn(btp)$_2$(dca)$_2$]$_n$ (2)*

To an aqueous solution (10 mL) of $Zn(ClO_4)_2 \cdot 6H_2O$ (37.3 mg, 0.1 mmol) was slowly added a methanol solution (10 mL) of btp (17.8 mg, 0.1 mmol) and Nadca (8.9 mg, 0.1 mmol) with constant stirring. After further stirring for *ca* 3 h at room temperature, the mixture was filtered. Upon slow evaporation of the filtrate at room temperature, colorless block-shaped crystals were grown within 10 days (yield: 58% based on Zn^{II}). Anal. Calcd for $C_9H_{10}N_9Zn_{0.50}$: C, 39.04%; H, 3.64%; N, 45.52%. Found: C, 39.23%; H, 3.71%; N, 45.58%. IR (KBr, cm^{-1}): 3125w, 2299s, 2224s, 2164vs, 1521s, 1374m, 1280m, 1135m, 989m, 649w, 511w.

2.4. *Synthesis of [Zn(btp)(NCS)$_2$] (3)*

Colorless block-shaped single crystals of **3** were obtained by adopting the same synthetic procedures as **2** only using NH_4NCS instead of Nadca (yield: 70% based on Zn^{II}). Anal. Calcd for $C_{36}H_{40}N_{32}S_8Zn_4$: C, 30.05%; H, 2.80%; N, 31.15%. Found: C, 30.24%; H, 2.68%; N, 31.31%. IR (KBr, cm^{-1}): 3114s, 3054w, 2091vs, 1624w, 1538s, 1282s, 1215m, 1135s, 1001w, 643w, 473w.

2.5. *Synthesis of [Mn(btp)$_2$(NCS)$_2$]$_n$ (4)*

$Mn(OAc)_2 \cdot 4H_2O$ (24.5 mg, 0.1 mmol), btp (17.8 mg, 0.1 mmol), NH_4NCS (15.2 mg, 0.2 mmol), and deionized water (10 mL) were sealed in a Teflon-lined reactor (23 mL) and heated at 160°C for 72 h. After the mixture was cooled to room temperature at a rate of 5.5°C h^{-1}, the mixture was filtered and left under the ambient environment for slow evaporation. Colorless block-shaped crystals suitable for X-ray diffraction analysis were obtained within 7 days (yield: 55% based on Mn^{II}). Anal. Calcd for $C_8H_{10}N_7S\,Mn_{0.50}$: C, 36.43%; H, 3.82%; N, 37.18%. Found: C, 36.51%; H, 3.85%; N, 37.09%. IR (KBr, cm^{-1}): 3109s, 2064vs, 1654w, 1517s, 1278s, 1200m, 1128vs, 979m, 887m, 674m, 529m, 472w.

2.6. *X-ray crystallography*

Diffraction intensities for the four complexes were collected on a Bruker Apex II CCD diffractometer at ambient temperature with Mo-Kα radiation ($\lambda = 0.71073$ Å) by ω–φ scan mode. Semiempirical absorption corrections were applied by using SADABS [13] and the program SAINT was used for integration of the diffraction profiles [14]. All structures were solved by direct methods using the SHELXS program of the SHELXTL package and refined with SHELXL [15]. The final refinement was performed by full-matrix least-squares methods on F^2 with anisotropic thermal parameters for all non-hydrogen atoms. The positions of hydrogens bonded to carbon were generated geometrically and allowed to ride on their parent carbons before the final cycle of refinement. Hydrogens attached to oxygen were first located in difference Fourier maps

and then placed in the calculated sites, and refined isotropically. For **1**, the perchlorate anion and C-4 of btp were orientation disordered. The chlorine and two sets of tetrahedral oxygens (Cl-1, O-1, O-2, Cl-1′ O-1′, O-2′) were refined with geometric constraints with occupancies of 41.3 and 58.7%, respectively. The methylene group of btp (C-4) is located on a two-fold rotation axis and varied between two positions with 50% occupancy. For **3**, two methylene groups (C-4 and C-5) of one btp ligand are disordered with occupation that refined to 61.0 and 39.0% for C-4–C-5 and C-4′–C-5′, respectively. Further crystallographic data and structural refinement parameters of complexes are summarized in table 1. Selected bond distances and angles are shown in table 2 and hydrogen-bond parameters were listed in table 3.

3. Results and discussion

3.1. *Synthesis and IR spectra*

Phase-pure crystals **1**–**3** were prepared by conventional evaporation due to the potentially explosive nature of $Zn(ClO_4)_2$. In contrast, **4** was obtained by the hydrothermal method. The molar ratio of reactant mixture for **4** (Mn^{II}/btp/$NCS^- = 1:1:2$) is slightly different from those in **2** and **3** [Zn^{II}/btp/NCS^- (dca^-) = 1:1:1]. Thus, it can be concluded that the preparation method and the molar ratio of the starting materials are important for isolation of the target complexes.

In IR spectra, absorption bands at 3131 cm^{-1} for **1**, 3125 cm^{-1} for **2**, 3114 cm^{-1} for **3**, and 3109 cm^{-1} for **4** should be assigned to C–H stretch of the triazole ring. Medium bands at 1510–1540 and 1270–1290 cm^{-1} for the four complexes are associated with C=C and C=N stretching vibrations of btp [6, 16, 17]. Additionally, **1** shows the characteristic bands for ionic perchlorate at 1095 and 620 cm^{-1} [18, 19]. For **2**, three sharp and strong stretching frequencies at 2299, 2224, and 2164 cm^{-1} are attributed to ν_{as} and ν_s (C≡N) combination modes indicating monodentate coordination of dca anion through an amide nitrogen [20, 21]. For **3** and **4**, similar characteristic bands for monodentate N-binding isothiocyanate are observed at 2091 and 473 in **3** and 2064 and 472 cm^{-1} in **4** [22, 23]. Thus, IR spectra agree with single-crystal structure determinations.

3.2. *Structural description of* $\{[Zn(btp)_3](ClO_4)_2\}_n$ *(1)*

Complex **1** crystallizes in the trigonal *P3c1* space group, including a 1-D triple-stranded cationic chain and two ClO_4^- anions for charge compensation. The Zn^{II} in the asymmetric unit is coordinated to six triazole nitrogens from six symmetry-related btp ligands, forming an ideal octahedral coordination geometry. The Zn–N bond length is 2.1893(17) Å and the N–Zn–N angles are 90° and 180° (see figure 1a and table 2). Btp adopts a *gauche–gauche* conformation with N···N distance of 5.3222(2) Å and the dihedral angle between the two triazole rings is 36.5°. Adjacent Zn^{II} ions are triply bridged by exo-bidentate bridging btp to generate a triple-stranded chain with nearest Zn···Zn separation of 7.7186 Å.

As shown in figure 1(b), adjacent chains are arranged in a hexagonal close-packed fashion in the crystallographic *ab* plane to lead to a 3-D supramolecular architecture,

Table 1. Crystal data and structure refinement for **1**–**4**.

	1	**2**	**3**	**4**
Empirical formula	$C_{3.50}H_5Cl_{0.33}N_3O_{1.33}Zn_{0.17}$	$C_9H_{10}N_9Zn_{0.50}$	$C_{36}H_{40}N_{32}S_8Zn_4$	$C_8H_{10}N_7SMn_{0.5}$
Formula weight ($g\,mol^{-1}$)	133.15	276.95	1438.96	263.76
Crystal system	Trigonal	Triclinic	Monoclinic	Triclinic
Space group	$P3c1$	$P\bar{1}$	$P2_1/c$	$P\bar{1}$
Unit cell dimensions (Å, °)				
a	11.0115(10)	8.0126(8)	9.3756(10)	7.8847(3)
b	11.0115(10)	8.5067(8)	8.6406(9)	8.6194(4)
c	15.4372(16)	10.7118(15)	19.0477(18)	9.6966(4)
α	90	111.758(2)	90	78.4850(10)
β	90	93.648(2)	105.315(4)	73.1140(10)
γ	120	115.0670(10)	90	67.8320(10)
Volume (Å^3), Z	1621.0(3), 12	592.73(12), 2	1488.3(3), 1	580.95(4), 2
Calculated density ($g\,cm^{-3}$)	1.637	1.552	1.606	1.508
Absorption coefficient (mm^{-1})	0.998	1.085	1.933	0.784
$F(000)$	820	284	728	271
Crystal size (mm^3)	$0.24 \times 0.23 \times 0.22$	$0.25 \times 0.24 \times 0.23$	$0.25 \times 0.23 \times 0.20$	$0.24 \times 0.23 \times 0.18$
θ range for data collection (°)	2.14–25.01	2.12–25.01	2.22–27.92	2.21–25.01
Limiting indices	$-13 \le h \le 12$; $-8 \le k \le 13$; $-17 \le l \le 18$	$-8 \le h \le 9$; $-10 \le k \le 9$; $-12 \le l \le 10$	$-12 \le h \le 10$; $-9 \le k \le 11$; $-24 \le l \le 25$	$-8 \le h \le 9$; $-5 \le k \le 10$; $-11 \le l \le 11$
Reflections collected	7622	3033	8908	2959
Independent reflection	961 [R(int) = 0.0191]	2082 [R(int) = 0.0078]	3468 [R(int) = 0.0154]	2028 [R(int) = 0.0072]
Max. and min. transmission	0.7957 and 0.8103	0.7796 and 0.7701	0.6799 and 0.6234	0.8717 and 0.8341
Data/restraints/parameters	961/12/98	2082/0/169	3468/6/200	2028/6/151
Goodness-of-fit on F^2	1.039	1.027	1.042	1.026
Final R indices [$I > 2\sigma(I)$]	$R_1 = 0.0346$, $wR_2 = 0.1033$	$R_1 = 0.0218$, $wR_2 = 0.0551$	$R_1 = 0.0398$, $wR_2 = 0.1046$	$R_1 = 0.0274$, $wR_2 = 0.0663$
R indices (all data)	$R_1 = 0.0374$, $wR_2 = 0.1075$	$R_1 = 0.0225$, $wR_2 = 0.0556$	$R_1 = 0.0493$, $wR_2 = 0.1113$	$R_1 = 0.0287$, $wR_2 = 0.0673$
Largest difference peak and hole (e Å^{-3})	0.464 and −0.328	0.161 and −0.218	0.664 and −0.902	0.366 and −0.472

[a] $R_1 = \Sigma||F_o|-|F_c||/|F_o|$. [b] $wR_2 = [\Sigma w(F_o^2-F_c^2)^2/\Sigma w(F_o^2)^2]^{1/2}$.

Table 2. Selected bond lengths (Å) and angles (°) for **1–4**.

1			
Zn(1)–N(3)	2.1893(17)	N(3)^{a}–Zn(1)–N(3)	180.0
N(3)^{a}–Zn(1)–N(3)^{b}	90.0		
2			
Zn(1)–N(3)	2.1555(13)	Zn(1)–N(7)	2.1515(14)
Zn(1)–N(6)^{b}	2.1744(13)		
N(7)^{a}–Zn(1)–N(7)	180.0	N(7)–Zn(1)–N(3)	90.17(5)
N(7)–Zn(1)–N(3)^{a}	89.83(5)	N(3)–Zn(1)–N(3)^{a}	180.0
N(7)^{a}–Zn(1)–N(6)^{b}	92.12(5)	N(7)–Zn(1)–N(6)^{b}	87.88(6)
N(3)–Zn(1)–N(6)^{b}	92.54(5)	N(3)–Zn(1)–N(6)^{c}	87.46(5)
N(6)^{b}–Zn(1)–N(6)^{c}	180.00(4)		
3			
Zn(1)–N(7)	1.941(3)	Zn(1)–N(8)	1.949(3)
Zn(1)–N(6)^{a}	1.994(2)	Zn(1)–N(3)	2.019(2)
N(7)–Zn(1)–N(8)	111.70(14)	N(7)–Zn(1)–N(6)^{a}	110.94(11)
N(8)–Zn(1)–N(6)^{a}	112.03(12)	N(7)–Zn(1)–N(3)	111.69(11)
N(8)–Zn(1)–N(3)	103.36(12)	N(6)^{a}–Zn(1)–N(3)	106.80(10)
4			
Mn(1)–N(7)	2.1783(16)	Mn(1)–N(6)^{b}	2.2863(14)
Mn(1)–N(3)^{a}	2.2806(14)		
N(7)^{a}–Mn(1)–N(7)	180.00	N(7)–Mn(1)–N(3)^{a}	89.29(6)
N(7)–Mn(1)–N(3)	90.71(6)	N(3)^{a}–Mn(1)–N(3)	180.0
N(7)^{a}–Mn(1)–N(6)^{b}	90.72(6)	N(7)–Mn(1)–N(6)^{b}	89.28(6)
N(3)^{a}–Mn(1)–N(6)^{b}	87.20(5)	N(3)–Mn(1)–N(6)^{b}	92.80(5)
N(6)^{b}–Mn(1)–N(6)^{c}	180.0	N(7)^{a}–Mn(1)–N(6)^{b}	90.72(6)

Symmetry codes for **1**: $^{a}-x, -y, -z$; $^{b}x-y, x, -z$; for **2**: $^{a}-x+2, -y+2, -z+1$; $^{b}x+1, y+1, z+1$; $^{c}-x+2, -y+1, z+1$; for **3**: $^{a}-x+1, -y, -z$; for **4**: $^{a}-x+1, -y+1, -z+1$; $^{b}x+1, y, z-1$; $^{c}-x, -y+1, -z+2$.

Table 3. Hydrogen-bonding parameters for **1–3**.

Donor–H···Acceptor	D–H	H···A (Å)	D···A (Å)	D–H···A (°)
1				
C3–H3B···O2	0.970	2.38	3.173(2)	138.86(3)
2				
C7–H7···N9^{a}	0.93	2.34	3.269(7)	173.67(6)
3				
C1–H1···N5^{a}	0.930	2.61	3.473(2)	156.33(7)
C7–H7···S2^{b}	0.930	2.66	3.564(4)	163.76(8)

Symmetry codes for **2**: $^{a}1+x, y, z$; for **3**: $^{a}-1+x, y, z$; $^{b}1-x, 1-y, -z$.

leaving the channel-like space occupied by lattice ClO_4^- through weak C3–H3B···O2 interactions (see table 3) [24]. Complex **1** is isomorphous to the recently reported Fe-btp-based complexes ($\{[Fe(btp)_3](ClO_4)_2\}_n$ and $\{[Fe(btp)_3](BF_4)_2\}_n$ [6]), although the metal ion and the lattice anions are different.

3.3. *Structural description of $[Zn(btp)_2(dca)_2]_n$ (2)*

With competitive coordination between btp and dca anion, **2** exhibits a neutral chain containing 20-membered $\{Zn_2(btp)_2\}$ loops and terminal dca^- anions in the

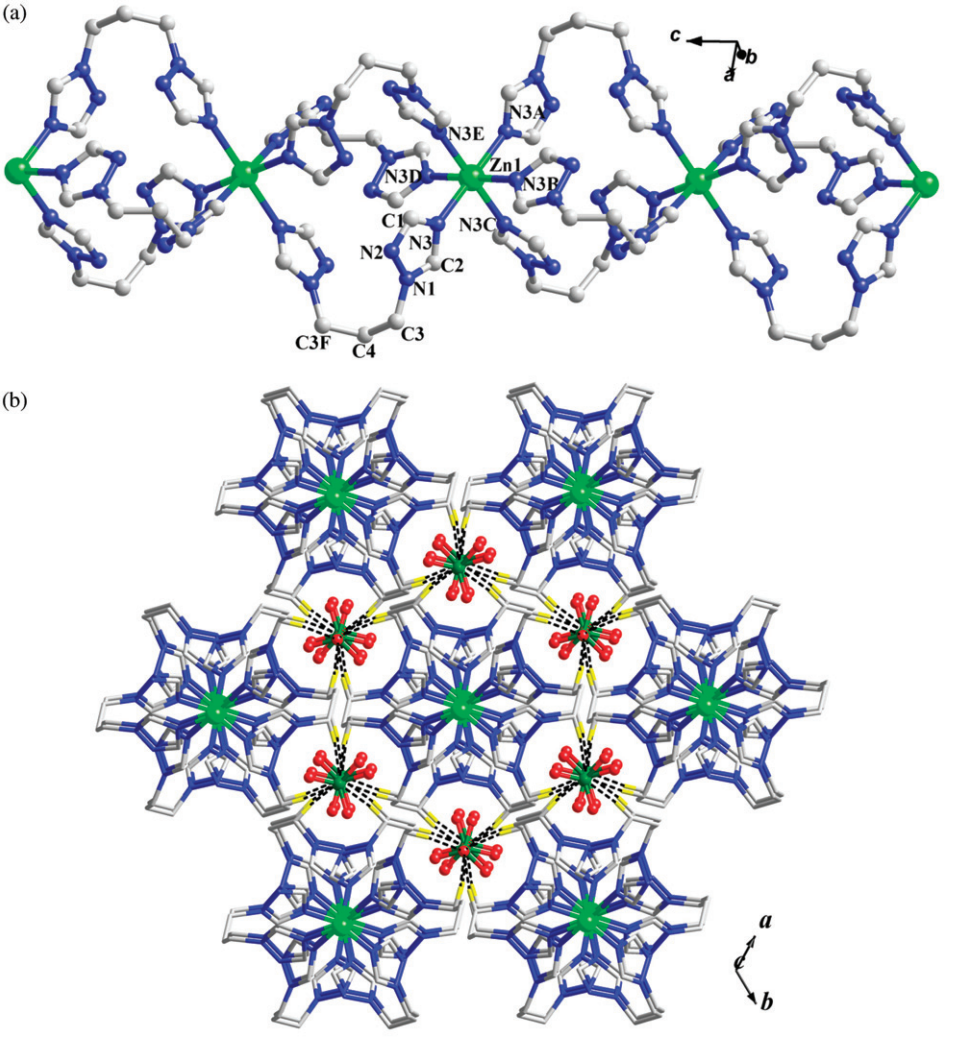

Figure 1. (a) The 1-D triple-stranded chain of **1** with atom labels of selected atoms in the asymmetric unit. (b) 3-D supramolecular network of **1** with weak C–H···OH-bonded ClO_4^- anions.

triclinic $P\bar{1}$ space group. Similar to **1**, the crystallographically unique Zn^{II} in the asymmetric unit is six-coordinated, equatorially by four triazole nitrogens and axially by two nitrile nitrogens from two *trans* dca^- coligands (see figure 2a). The Zn–N_{btp} distances are 2.1555(13) and 2.1745(13) Å, slightly longer than Zn–N_{dca} distances [2.1515(14) Å, see table 2]. The dca^- is bent with a C(8)–N(8)–C(9) bond angle of 120.856(8)°. The btp exhibits a *trans–trans* conformation with the longest N···N distance within the btp ligand of 8.1593(9) Å and dihedral angles between the two triazole rings of 75.26°. Two btp molecules join adjacent Zn^{II} ions in an exo-bidentate bridging mode to form 20-membered $\{Zn_2(btp)_2\}$ loops, in which the Zn···Zn separation across the bridging btp is 10.9339(11) Å, much longer than in **1** (7.7186 Å). The relative longer Zn···Zn separation for **2** results from intrinsic flexibility of btp.

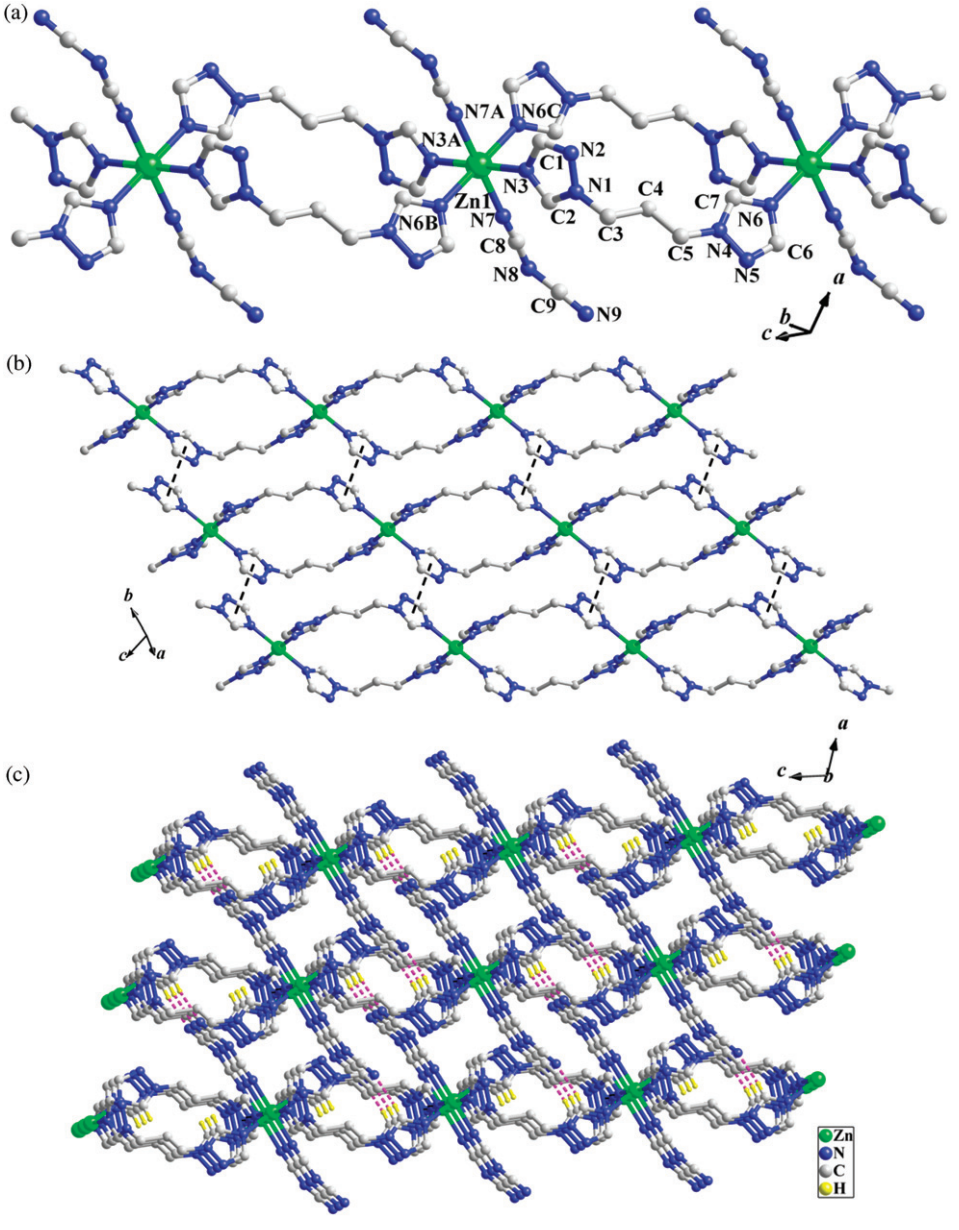

Figure 2. (a) The 1-D double-stranded chain of **2** with atom labels of selected atoms in the asymmetric unit. (b) The 2-D supramolecular structure of **2** formed by interchain $\pi\cdots\pi$ stacking interaction (terminal dca ligands are omitted for clarity). (c) 3-D supramolecular framework of **2** assembled from weak C–H···N hydrogen-bonding interaction.

As shown in figure 2(b), adjacent chains are packed into a 2-D layer by strong face-to-face π–π stacking interactions between triazole rings of btp. The centroid–centroid distance is 3.6167 Å and the dihedral angle between rings is 0.0°. Furthermore, weak C–H···N hydrogen-bonds (see table 3) between carbon of triazole ring and nitrogen of dca^- generate a 3-D supramolecular network of **2** (figure 2c).

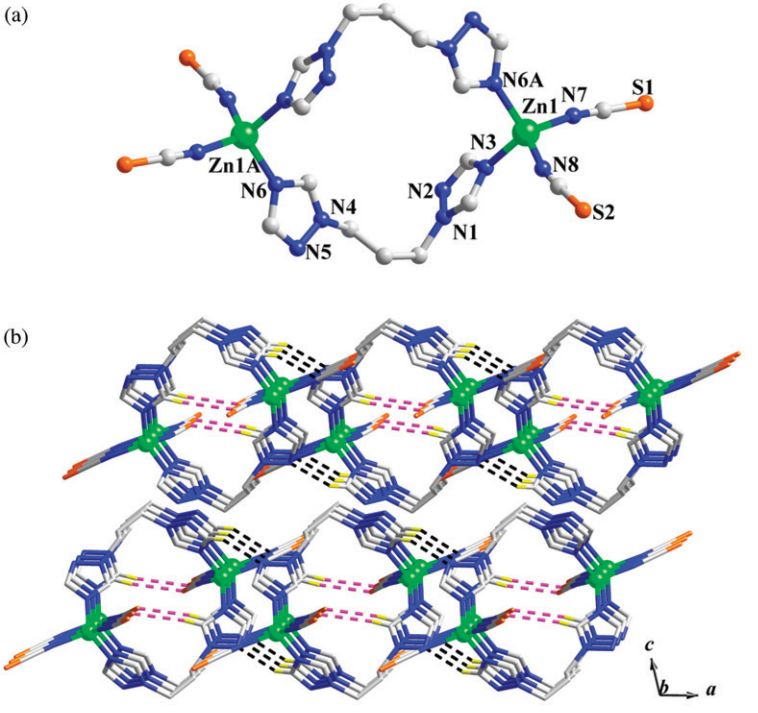

Figure 3. (a) Binuclear structure of **3** with atom labels in the asymmetric unit. (b) 2-D supramolecular layer formed by C–H···N and C–H···S hydrogen-bonding interactions.

3.4. *Structural description of [Zn(btp)(NCS)$_2$]$_n$ (3)*

Different from the polymeric structures of **1** and **2**, **3** is a discrete centrosymmetric bimetallic complex, which is significantly tuned by the coordination polyhedron of Zn^{II}. As shown in figure 3(a), two symmetry-related Zn^{II} centers are four-coordinated, surrounded by two exo-bidentate bridging btp ligands and two N-monodentate NCS^-. As a result, a closed 20-membered $\{Zn_2(btp)_2\}$ metallomacrocycle is generated with Zn···Zn separation of 9.2543(8) Å. Additionally, Zn–N_{btp} bond lengths are *ca* 0.05 Å longer than those of Zn–N_{NCS} (see table 2). The terminal NCS^- is almost linear with N–C–S angles of 177.753(338) and 179.229(302). Btp ligand is *trans–gauche* conformation with the longest N···N distance of 7.1485(41) Å and the dihedral angle of two triazole rings 82.6(3)°.

As shown in figure 3(b), the discrete binuclear structures are further connected into a 2-D sheet through weak C–H···N and C–H···S hydrogen-bonds (see table 3) in the crystallographic *ac*-plane; no significant interaction (hydrogen-bond or aromatic stacking) can be found between adjacent sheets.

3.5. *Structural description of [Mn(btp)$_2$(NCS)$_2$]$_n$ (4)*

Although the metal ion and the coligand of **4** are different from those of **2**, **4** also crystallizes in triclinic $P\bar{1}$ space group, exhibiting an infinite chain with 20-membered

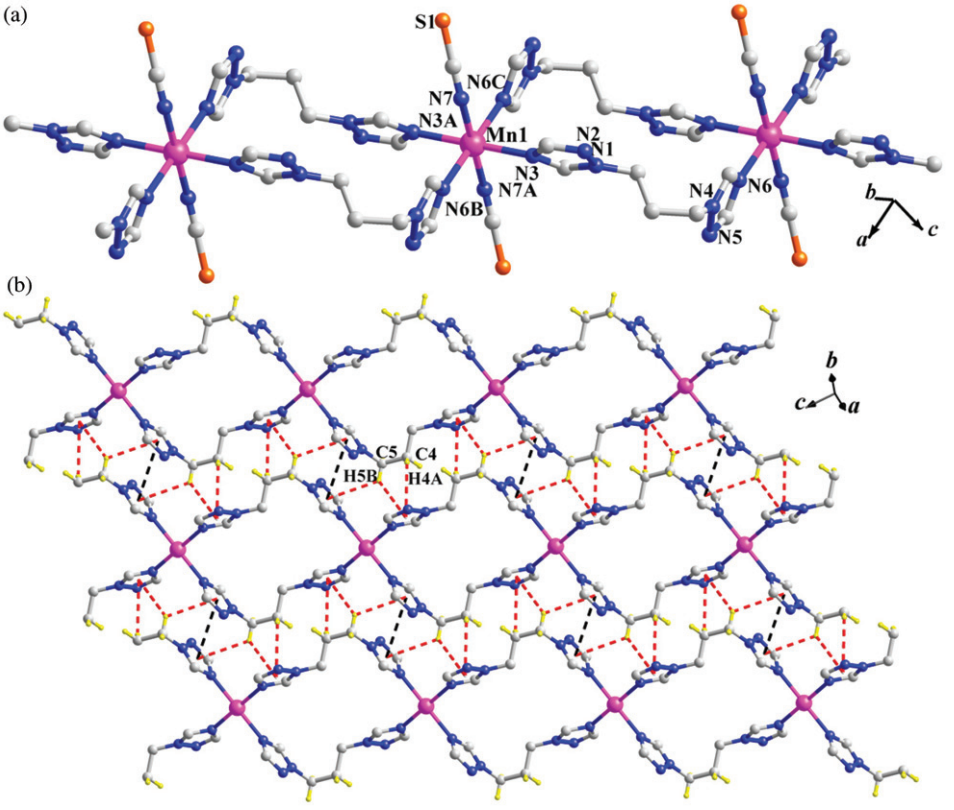

Figure 4. (a) The 1-D double-stranded chain of **4** with atom labels for selected atoms in the asymmetric unit. (b) The 2-D supramolecular structure of **4** formed by interchain C–H$\cdots\pi$ and $\pi\cdots\pi$ stacking interactions (terminal NCS^- ligands are omitted for clarity).

$\{Mn_2(btp)_2\}$ loops. Additionally, **4** is also iso-structural with $[Co(btp)_2(NCS)_2]_n$ [2]. The crystallographically independent Mn^{II} is octahedral with the equatorial plane occupied by four nitrogens of triazoles and the axial positions by two *trans* NCS^-. The Mn–N bond lengths are 2.1785(16)–2.2863(14) Å, slightly longer than those of $[Co(btp)_2(NCS)_2]_n$ [2] [2.101(2)–2.191(2) Å] because of the different metal radii. The monodentate binding mode and linear [$\angle$N(7)C(8)S(1) = 177.654(3)°] NCS^- is almost the same as for **3**; the Mn$\cdots$Mn separation is 10.5725(3) Å.

Although the btp shows a *trans–gauche* conformation, the geometrical parameters are different from those in **3** with the longest N3$\cdots$N6 distance of btp in **4** 7.5613(3) Å and the dihedral angle of the two triazole rings 74.04° [7.148(16) Å and 83.475° in **3**]. The specific orientation of btp is influenced by new weak intermolecular C–H$\cdots\pi$ interactions, absent in **2**.

As shown in figure 4(b), in addition to inter-chain π–π interactions (the centroid-to-centroid distance is 3.738 Å and the dihedral angle between the triazole rings is 0.0°), three-fold C–H$\cdots\pi$ interactions between the methylene group of propane and triazole rings of btp can be observed, further consolidating the 2-D supramolecular layer. The distances *d* (H$\cdots$Cg) and C-donor *D* (C$\cdots$Cg) to the center of the triazole ring (Cg) are

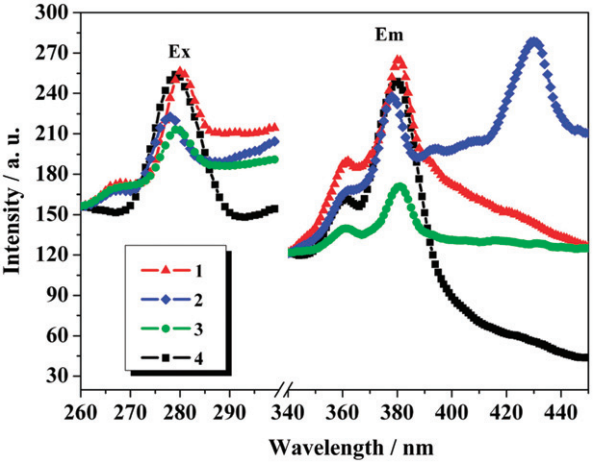

Figure 5. Solid luminescent spectra of **1**–**4**.

3.0104(1), 3.0853(1), 3.2618(1) and 3.5665(1), 3.6681(1), 3.9207(2) Å, and the angle θ(C–H···Cg) are 117.668(4)°, 120.025(5)°, 126.815(5)°, respectively.

3.6. *Thermal stability of the complexes*

Thermogravimetric analysis suggests that the presence of the coligand in **2–4** significantly changes the thermal stability of the resulting complexes. In comparison to **1** without coligand, polymeric **2** and **4** with dca^- and NCS^- coligands decompose at 174 and 222°C, respectively, much lower than for **1** without coligand (260°C). The discrete binuclear structure **3** exhibits the highest stability (262°C). Upon further heating, each complex exhibits two continuous weight-loss processes, corresponding to removal of btp and coligands for **2–4** and btp and lattice ClO_4^- anion for **1**.

3.7. *Luminescent properties*

Luminescences of solid **1–4** at room temperature, figure 5, show **1–3** having similar emissions at *ca* 380 nm with different intensity upon excitation at 280 nm; **2** displays an additional emission at 430 nm upon excitation at 278 nm. Emission of the free btp in the solid state displays strong emission at 381 nm, upon excitation at *ca* 280 nm. Thus, the emissions at 378 nm result from intraligand charge transfer with the slight shift ascribed to different conformations of btp. For **2**, the strong emission at 430 nm results from ligand-to-metal charge transfer.

4. Conclusion

Four Zn^{II}/Mn^{II} complexes with btp core ligand have been isolated by selectively introducing small anions as coligands. The overall structures vary from triple-stranded

chain for **1**, double-stranded chain for **2** and **4** and discrete binuclear structure for **3**. Thermal stability of the target complexes is also significantly influenced by the coligands. Strong emissions for the complexes in the solid state suggest applications as functional materials.

Supplementary material

Crystallographic data (excluding structure factors) for the crystal structures reported in this article have been deposited with the Cambridge Crystallographic Data Center (CCDC Nos. 734374–734377). This material can be obtained free of charge via www.ccdc.cam.ac.uk/conts/retrieving.html (or from the CCDC, 12 Union Road, Cambridge CB2 1EZ, UK; Fax: +44 1223 336033; Email: deposit@ccdc.cam.ac.uk).

Acknowledgements

The present work was financially supported by the National Natural Science Foundation of China (20703030, 20871092), the Key Project of Chinese Ministry of Education (Grant No. 209003), and the Program for New Century Excellent Talents in University (NCET-08-0914), which are gratefully acknowledged.

References

[1] G.A.V. Albada, R.C. Guijt, J.G. Haasnoot, M. Lutz, A.L. Spek, J. Reedijk. *Eur. J. Inorg. Chem.*, 121 (2000).
[2] Q.H. Zhao, H.F. Li, X.F. Wang, Z.D. Chen. *New J. Chem.*, **26**, 1709 (2002).
[3] X.Y. Wang, B.L. Li, X. Zhu, S. Gao. *Eur. J. Inorg. Chem.*, **16**, 3277 (2005).
[4] J.G. Ding, X.G. Liu, B.L. Li, L.Y. Wang, Y. Zhang. *Inorg. Chem. Commun.*, **11**, 1079 (2008).
[5] X. Zhu, X.G. Liu, B.L. Li, Y. Zhang. *Cryst. Eng. Comm.*, **11**, 997 (2009).
[6] F.M. Effendy, C. Pettinari, R. Pettinari, M. Ricciutelli, B.W. Skelton, A.H. White. *Inorg. Chem.*, **43**, 2157 (2004).
[7] L. Yi, X. Yang, T.B. Lu, P. Cheng. *Cryst. Growth Des.*, **5**, 1215 (2005).
[8] Z.G. Gu, Y.F. Xu, X.H. Zhou, J.L. Zuo, X.Z. You. *Cryst. Growth Des.*, **8**, 1306 (2008).
[9] (a) X.G. Liu, K. Liu, Y. Yang, B.L. Li. *Inorg. Chem. Commun.*, **11**, 1273 (2008); (b) X. Zhu, K. Liu, Y. Yang, B.L. Li, Y. Zhang. *J. Coord. Chem.*, **62**, 2358 (2009).
[10] (a) Y.Y. Liu, L. Yi, B. Ding, Y.Q. Huang, P. Cheng. *Inorg. Chem. Commun.*, **10**, 517 (2007); (b) Y.Y. Liu, B. Ding, E.C. Yang, X.J. Zhao, X.G. Wang. *J. Coord. Chem.*, **62**, 1623 (2009); (c) B. Ding, E.C. Yang, X.J. Zhao, X.G. Wang. *J. Coord. Chem.*, **62**, 287 (2009).
[11] X.S. Qu, L. Xu, G.G. Gao, F.Y. Li, Y.Y. Yang. *Inorg. Chem.*, **46**, 4775 (2007).
[12] X. Zhu, H.Y. Ge, Y.M. Zhang, B.L. Li, Y. Zhang. *Polyhedron*, **25**, 1875 (2006).
[13] G.M. Sheldrick. *SADABS: Program for Empirical Absorption Correction of Area Detector Data*, University of Göttingen, Germany (1996).
[14] Bruker AXS. *SAINT Software Reference Manual*, Madison, WI (1998).
[15] (a) G.M. Sheldrick. *SHELXL-97, Program for X-ray Crystal Structure Refinement*, Göttingen University, Göttingen, Germany (1997); (b) G.M. Sheldrick. *SHELXS-97, Program for X-ray Crystal Structure Solution*, Göttingen University, Göttingen, Germany (1997).
[16] L.J. Bellamy. *The Infrared Spectra of Complex Molecules*, Wiley, New York (1958).
[17] G.B. Deacon, R.J. Phillips. *Coord. Chem. Rev.*, **33**, 227 (1980).
[18] K. Nakamoto. *Infrared and Raman Spectra of Inorganic and Coordination Compounds*, 4th Edn, Wiley, New York (1986).

[19] S. Chowdhury, M.G.B. Drew, D. Datta. *Inorg. Chem. Commun.*, **6**, 1014 (2003).
[20] M. Du, X.J. Zhao, S.R. Batten, J. Ribas. *Cryst. Growth Des.*, **5**, 901 (2005).
[21] H. Köhler, A. Kolbe, G. Lux. *Z. Anorg. Allg. Chem.*, **428**, 103 (1977).
[22] L.R. Groeneveld, G. Vos, G.C. Verschoor, J. Reedijk. *J. Chem. Soc., Chem. Commun.*, 620 (1982).
[23] J.G. Ding, H.Y. Ge, Y.M. Zhang, B.L. Li, Y. Zhang. *J. Mol. Struct.*, **782**, 143 (2006).
[24] J. Schweifer, P. Weinberger, K. Mereiter, M. Boca, C. Reichl, G. Wiesinger, G. Hilscher, P.J van Koningsbruggen, H. Kooijman, M. Grunert, W. Linert. *Inorg. Chim. Acta*, **339**, 297 (2002).